Int. J. Heat Mass Transfer. Vol. 36, No. 18, pp. 4365–4373, 1993
Printed in Great Britain

0017–9310/93 $6.00 + 0.00

Numerical study of laminar heat transfer with temperature dependent fluid viscosity in a 2:1 rectangular duct

SEHYUN SHIN, YOUNG I. CHO, WILLIAM K. GRINGRICH† and WEI SHYY‡
Department of Mechanical Engineering and Mechanics, Drexel University, Philadelphia, PA 19104, U.S.A.

(*Received* 9 *December* 1992 *and in final form* 24 *May* 1993)

Abstract—The present study investigates the influence of variable viscosity of temperature-dependent fluids on the laminar heat transfer and friction factor in a 2:1 rectangular duct. The H_1 thermal boundary condition corresponding to axially constant heat flux and peripherally constant temperature was adopted for a top-wall-heated configuration. The governing conservation equations of mass, momentum, and energy were solved using a finite volume method, and the range of the Prandtl number was from 7 to 15000. The present numerical results of local Nusselt numbers for oil showed 70–80% enhancement over those of a constant property fluid and 40–50% enhancement over water, and gave excellent agreement with recent experimental results [*Int. J. Heat Mass Transfer* **35**, 641–648 (1992)]. The heat transfer enhancement from the heated top wall was due to an increased velocity gradient near the wall. The study proposes a new correlation for local Nusselt numbers in the 2:1 rectangular duct, which covers both thermally developing and thermally fully developed regions. Consequently, a temperature-dependent viscous fluid with a non-circular duct is proposed for use in the design of a liquid cooling module for the computer industry and in compact heat exchangers in general.

1. INTRODUCTION

A STRONG interest in the flow of temperature-dependent viscous fluids in rectangular ducts is based on the potential heat transfer enhancement associated with the temperature-dependent viscosity, as demonstrated by a recent report by Xie and Hartnett [1]. This interest stems from the practical use of these fluids in heat exchangers and in the cooling of electronics. For most fluids, the physical properties of specific heat, thermal conductivity, and density are relatively independent of temperature, but the viscosity decreases very markedly with temperature. For example, the viscosity of glycerin decreases from 1.85 Pa s at 290 K to 0.21 Pa s at 320 K, whereas that of ethylene glycol decreases from 0.0247 Pa s at 290 K to 0.00757 Pa s at 320 K [2]. Thus, viscosity is very temperature-dependent even for water. This viscosity variation with temperature alters velocity profiles, particularly where there is an uneven thermal boundary condition such as a heated top wall in a rectangular duct. Consequently, the heat transfer and friction coefficients will be different from the values obtained with a fluid whose viscosity is independent from temperature variations.

2. BACKGROUND AND OBJECTIVE

Many studies have reported variable-property analyses in the literature [1–17]. The general effect of the variation of the transport properties with temperature on flow and heat transfer was to increase the velocity and temperature gradients. This effect depends on the type of duct geometry and thermal boundary condition (i.e. whether it is symmetric or asymmetric).

For a circular duct, where one expects a symmetric heating at the wall, Sieder and Tate [5] experimentally investigated the effect of variable viscosity on heat transfer in both heating and cooling situations. Traditionally, the temperature effect on flow and heat transfer were shown in the following equations:

$$Nu/Nu_{cp} = (\eta_b/\eta_w)^n \tag{1}$$

and

$$f/f_{cp} = (\eta_b/\eta_w)^{-m}. \tag{2}$$

Sieder and Tate [5] reported that the n value in equation (1) was 0.14, and the m value in equation (2) was 0.25 for laminar flow. Deissler [6] solved the same problem analytically and reported $n = 0.14$ and $m = 0.54$. Yang [7] studied the variable viscosity effect on heat transfer in developing and fully developed regions with both constant wall temperature and heat flux boundary conditions in a circular tube; he reported that the n value was 0.11. Shannon and Depew [8] numerically studied fully developed heat transfer with a constant heat flux boundary condition in a circular tube, but their predictions differed from Yang's, particularly in the entrance region. Shannon and Depew reported that at the entrance of the tube, n was approximately 0.3 and decreased to 0.14 in the fully developed region. Oskay and Kakaç [9] studied the heat transfer of a mineral oil flowing through a circular tube with constant heat flux at the wall and

† Deceased (17 February 1992).
‡ University of Florida, Department of Aerospace Engineering, Mechanics and Engineering Science, Gainesville, FL 32611, U.S.A.

NOMENCLATURE

$\bar{C}_p$	specific heat of fluid
$\bar{D}_h$	hydraulic diameter
f	fanning friction factor, $(-\mathrm{d}\bar{P}/\mathrm{d}\bar{z})/[\bar{D}_h/(2\bar{\rho}\bar{V}_{avg}^2)]$
$\bar{g}$	gravity
Gz	Graetz number, $(Re\,Pr\,\bar{D}_h)/\bar{z}$
$\bar{h}_{fc}$	forced convection heat transfer coefficient
$\bar{K}_f$	thermal conductivity of fluid
m	exponent introduced in equation (2)
n	exponent introduced in equation (1)
Nu	Nusselt number, calculated at the heated top wall
Pe	Peclet number, $Re\,Pr$
Pr	Prandtl number, $\bar{\eta}_{ref}\bar{C}_p/\bar{K}_f$
$\bar{q}''$	heat flux
Re	Reynolds number, $(\bar{\rho}\bar{V}_{avg}\bar{D}_h)/\bar{\eta}_{ref}$
T	non-dimensional temperature, $(\bar{T}-\bar{T}_i)/(q''\bar{D}_h/\bar{K}_f)$
$\bar{T}_i$	fluid inlet temperature
$\bar{T}_w$	wall temperature
$\bar{v}_z$	axial velocity
v_z	non-dimensional axial velocity, $\bar{v}_z/\bar{v}_{avg}$
$\bar{V}_{avg}$	average axial velocity
$\bar{x}$, $\bar{y}$	axes of Cartesian coordinate system
x, y	non-dimensional axes of Cartesian coordinate, $\bar{x}/\bar{D}_h$, $\bar{y}/\bar{D}_h$
x^*, y^*	non-dimensional lateral and vertical distance, $\bar{x}/\bar{x}_0$, $\bar{y}/\bar{y}_0$
$\bar{z}$	axial distance
z	non-dimensional axial distance, $\bar{z}/(\bar{D}_h\,Re\,Pr)$.

Greek symbols

Γ	aspect ratio (i.e. ratio of width to height $= y_0/x_0$)
ζ	constant viscosity-variation parameter introduced in equation (6)
$\bar{\eta}_{ref}$	reference viscosity (at inlet temperature of 20 C)
η	non-dimensional viscosity, $\bar{\eta}(\bar{y})/\bar{\eta}_{ref}$
μ	Newtonian viscosity
$\mu_{b,avg}$	average bulk viscosity of fluid, evaluated at $1/2(T_i+T_o)$
ϕ	non-dimensional temperature, $\bar{T}/[(\bar{q}''_{ref}\bar{D}_h)/\bar{K}_f]$.

Subscripts

b	bulk
b,avg	bulk average
cp	constant property
fc	forced convection
i	inlet
o	outlet
w	wall.

Superscripts

$\bar{}$	dimensional quantities.

reported that the n value was 0.152. Test [10] analytically and experimentally studied laminar heat transfer for the constant wall temperature boundary condition. He concluded that because of the changes in velocity profile due to variable viscosity, the radial convection term should be retained in the energy equation. Rosenberg and Hellums [11] studied the developing laminar flow with the Prandtl number ranging from 2 to 1000 and reported that results for the high Prandtl number agreed with those of $Pr = 2$ within 20%.

Oliver and Rao [12] questioned the validity of equation (1) and proposed that the correction for the variable viscosity should include some dependence on the Graetz number to fit their data better for a highly viscous oil (Valvata-85). These results were qualitatively in agreement with the analytical results of Joshi and Bergles [13]. When the inlet effect was considered by means of the Graetz number, the exponent of the viscosity ratio correction was found to be considerably larger than the fully developed value [14].

Turning to a non-circular duct geometry, Lyutikas and Zhukauskas [3] analytically investigated the influence of variable viscosity on the laminar heat transfer in a flat duct in a thermally developing flow region, and reported that the n value in equation (1) was 0.167. Preiningerova and Allen [15] conducted a similar study by varying heat flux and mass flow rate and reported that the higher Nusselt number was shown to have a larger heat flux at the same mass flow rate, and a small mass flow rate at a same heat flux. Butler and McKee [4] analytically expressed the velocity profile in a fully developed flow with temperature-dependent viscous fluids in top-wall-heated rectangular ducts with aspect ratios of 0.5, 5 and 10, but did not report the m value or any heat transfer results. Hwang and Hong [16] obtained an analytical solution and experimental results using a rectangular duct for the constant wall temperature condition with ethylene glycol; they reported that the Nusselt numbers increased by 15–20% from the values of constant property fluid. Kakaç [17] summarized the values of n and m of five important studies.

Recently, Xie and Hartnett [1] experimentally studied the laminar heat transfer performance of a mineral oil in a 2:1 rectangular duct with a top-wall-heated thermal boundary condition (i.e. H_1). They reported that the local Nusselt numbers from the heated top wall increased by approximately 30–40% over the values for water, a phenomenon that was

attributed to a secondary flow resulting from an asymmetric velocity profile associated with the variable viscosity of the mineral oil [1].

The objective of the present study is to investigate numerically the effect of variable viscosity on the local laminar heat transfer performance of temperature-dependent fluids in a 2:1 rectangular duct in order to examine flow and temperature distributions in the rectangular duct more closely. In order to delineate the effect of the secondary flow at the corner of the rectangular duct, an axially parallel flow is assumed such that the axial velocity, $v_z(x, y, z)$, is the only non-zero velocity component. Thus, the present calculation represents the case of a thermally developing but axially parallel flow with a heated top wall in the 2:1 rectangular duct. Note that the top-wall-heated rectangular duct is one of the basic designs for a liquid cooling module for the computer industry.

3. PROBLEM DESCRIPTION AND ASSUMPTIONS

A schematic diagram of the system under consideration is shown in Fig. 1. Fluid enters the duct with a fully developed parabolic velocity profile and a uniform temperature T_i. The H_1 thermal boundary condition corresponding to axially constant heat flux and peripherally constant temperature is adopted, i.e. top-wall-heated, with other walls adiabatic. In order to simplify the computational model, the following treatments are incorporated:

(1) Constant fluid properties, except for the viscosity, which is exponentially dependent on the temperature.

(2) No axial conduction of thermal energy, which requires a large Peclet number (i.e. the product of the Reynolds number, Re, and the Prandtl number, Pr).

(3) Negligible viscous dissipation of thermal energy, which requires that the Brinkman number, Br, a measure of the magnitude of the viscous dissipation, be very small.

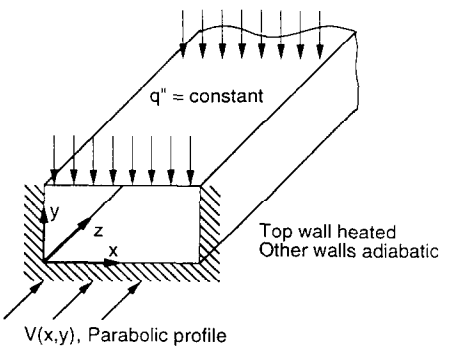

FIG. 1. Hydrodynamic and thermal boundary conditions. A parabolic velocity profile was used at the inlet of the rectangular duct.

(4) No axial velocity gradient, $\partial v_z/\partial z$, in the axial momentum equation.

4. FORMULATION AND NUMERICAL TECHNIQUES

The non-dimensional forms of the conservation equations of mass, momentum, and energy for an axially parallel and thermally developing flow in a rectangular duct are given as follows:

Continuity

$$\int\int v_z \, dx \, dy = 1.0 \tag{3}$$

Axial momentum

$$\frac{\partial}{\partial x}\left(\eta(T)\frac{\partial v_z}{\partial x}\right)+\frac{\partial}{\partial y}\left(\eta(T)\frac{\partial v_z}{\partial y}\right)+2f*Re=0 \tag{4}$$

Energy

$$v_z\frac{\partial \phi}{\partial z}=\left[\frac{\partial^2\phi}{\partial x^2}+\frac{\partial^2\phi}{\partial y^2}\right] \tag{5}$$

which are based on the reference temperature, i.e. inlet temperature 20°C. In order to assess the role of viscosity variation on the development of the flow field, the temperature-dependent viscosity is employed. Viscosity should have a dramatic effect on the flow field of temperature-dependent fluids, and the magnitude of the effect depends on types of fluids, duct geometry, mass flow rate [15], and relative magnitude of heat flux.

The temperature dependence of viscosity is described by an exponential model, which, in dimensionless form, is

$$\eta = C_1 10^{(\zeta T)} \tag{6}$$

where T is a dimensionless temperature introduced for H_1 boundary condition, defined as

$$T=\frac{(\bar{T}-\bar{T}_i)}{(q''\bar{D}_h/\bar{K}_f)} \tag{7}$$

and ζ represents the slope of the viscosity curve, i.e. η vs T, which becomes negative in the case of heating. The values of ζ for various fluids are listed in Table 1, which also shows the ratios of density, specific heat, thermal conductivity, and viscosity at two different temperatures, i.e. at 20 and 50°C, and the Prandtl number. The viscosity ratio for glycerin is much larger than that for mineral oil. However, the value of ζ for glycerin is nearly the same as that for mineral oil. This is due to the difference in thermal conductivities of the two fluids used in the dimensionless temperature; $k = 0.15$ W m^{-1} K^{-1} for mineral oil and $k = 0.286$ W m^{-1} K^{-1} for glycerin. Hence, the present numerical study with $\zeta = 11.1$ represents the case for both mineral oil and glycerin. The Prandtl number covered in the present study ranges from 7 to 15000. The product of the Fanning friction factor, f, and the

Table 1. The ratio of some physical properties of various fluids at temperature of 20 C and 50 C

Fluid	(ρ_{20}/ρ_{50})	(C_{p20}/C_{p50})	(K_{t20}/K_{t50})	(η_{20}/η_{50})	ζ	Pr_{20}
Water	1.011	1.000	0.940	1.816	−1.17	6.9
Ethylene glycol	1.021	0.945	0.961	3.263	−6.09	209.2
Mineral oil (10-NF)†	1.022	0.933	1.027	3.592	−11.1	511.5
Engine oil	1.021	0.937	1.014	7.085	−13.0	10853.0
Glycerin	1.015	0.923	0.997	8.809	−11.1	12616.0

For which ζ is a viscosity-variation parameter, which is constant for a given fluid.
† From J. J. Powell, Inc. (Amoco Oil Products), P.O. Box 30, Philipsburgh, PA 16866, U.S.A.

Reynolds number, Re, represents a momentum source term in the non-linear axial momentum equation [18, 19].

Boundary conditions

Both the velocity and a generalized form of the thermal boundary conditions in non-dimensional form are given below. The no-slip boundary condition is applied along the periphery of the duct for the axial velocity component.

Axial momentum:

$$v_z(0, y) = 0 \tag{8}$$

$$v_z\left(\frac{\Gamma+1}{2\Gamma}, y\right) = 0 \tag{9}$$

$$v_z(x, 0) = 0 \tag{10}$$

$$v_z\left(x, \frac{\Gamma+1}{2}\right) = 0. \tag{11}$$

Energy:

$$C_1\phi + C_2\left[\left(\frac{dy}{ds}\right)\frac{\partial\phi}{\partial x} - \left(\frac{dx}{ds}\right)\frac{\partial\phi}{\partial y}\right] = C_3 \tag{12}$$

where

$$ds = [(dx)^2 + (dy)^2]^{1/2}$$

$$C_1 = I_1$$

$C_2 =$

$$\begin{cases} 1: \text{constant temperature boundary condition} \\ 0: \text{non-constant temperature boundary condition} \end{cases} \tag{13}$$

$$C_3 = I_1\phi_{\text{given}} + I_2 q'' \tag{14}$$

$I_1 =$

$$\begin{cases} 1: \text{constant temperature boundary condition} \\ 0: \text{non-constant temperature boundary condition} \end{cases} \tag{15}$$

$$I_2 = \begin{cases} 1: \text{constant heat flux boundary condition} \\ 0: \text{constant temperature boundary condition.} \end{cases} \tag{16}$$

Solution methodology

Solutions to the problem defined by the equations above were obtained numerically by finite volume procedures [20, 21]. A second-order accurate difference scheme was employed for the diffusion terms, while the second-order upwinding scheme [22] was employed for the convective term in the energy equation for all interior nodal points. For the near-boundary control volumes, no special discretization equation was required, since the boundary condition data could be directly employed at the boundary face. This convenient property arose because the grid points were placed at the centers of the control volume. In the calculation of the rate of deformation tensor, a second-order central difference scheme was employed for the interior nodes, while a first-order difference between the near-boundary and boundary nodal points was employed for the near-boundary control volumes.

A fully implicit solution technique was adopted for both the momentum and energy equations at any given axial location. At a given axial location, the successive line underrelaxation (SLUR) procedure [23] was employed for the solution of the implicit finite difference form of the governing equations. Since the energy equation is parabolic in the axial direction, a marching solution was employed. For the momentum equation, a predictor/corrector method was developed by employing SLUR for the inner iteration solver for a given $f * Re$ product in combination with the Van Wijngaarden–Dekker–Brent searching methodology for the outer iteration [18].

Equations (4) and (5) were solved by an iterating procedure in which the temperature distribution obtained for constant property assumption was used as the first approximation. Then, using the appropriate viscosity variation with temperature, as given in equation (6), the momentum equation was solved to yield the second approximation for the velocity distribution. This improved velocity distribution was employed in the calculation of the energy equation to yield the second approximation for the temperature distribution. The procedure was repeated until the velocity and temperature distributions changed less than 0.1%, as compared to the values in the previous step.

Convergence for the SLUR procedure was monitored by examining how well the discretization equa-

tion was satisfied by the current values of the dependent variables. For each grid point, the residual R was calculated as

$$R = \sum a_{nb}\Theta_{nb} + b - a_p\Theta_p \qquad (17)$$

where Θ_{nb} are the neighboring dependent variables, a_{nb} are the coefficients corresponding to these neighboring dependent variables, b represents the other terms in the governing finite difference equations, Θ_p is the current nodal point dependent variable, and a_p is the coefficient corresponding to Θ_p. The convergence criteria for the SLUR method required that for any given grid point, the absolute value of the residual $|R|$ be less than 10^{-4}.

5. RESULTS AND DISCUSSION

The current numerical study used the properties of density, thermal conductivity, specific heat, and viscosity of three different fluids as reported in the literature [1, 9]. For mineral oil, the values reported by Xie and Hartnett were used so that our results could be compared with their experimental heat transfer results [1]. To double check the temperature-dependent viscosity of the mineral oil (10-NF, Amoco), the viscosity of the oil was measured over a range of temperature using a Brookfield viscometer. The experimental uncertainty of viscosity measurement was less than 3% and the precision limit of temperature measurement was ± 0.05°C. The effect of these uncertainties on the numerical simulation was less than 4%. Our viscosity results, represented by solid circles in Fig. 2, gave good agreement with the data reported by Xie and Hartnett [1], represented as solid squares in Fig. 2.

Prior to presenting any numerical solutions of interest, the appropriate grid size was assessed. On a uniform grid, a number of simulations were carried out by varying grid sizes in order to solve the continuity and momentum equations for a constant property fluid—a case where well-established values of $f * Re$ are available. The exact analytical value of $f * Re$ is 15.54806, Shah and London's value is 15.55733, and the current value with 62×62 grid was 15.52953. The values of $f * Re$ became independent of grid sizes beyond 42×42. Hence, a 42×42 grid size was employed for all the calculations presented in the present study. Appropriate axial space-marching steps along the axial direction were chosen from 10^{-4} to 10^{-2} for the energy equation.

Figure 3(a) shows the effect of the variable viscosity of mineral oil on temperature profiles in the thermally developing region, where two temperature profiles calculated for the mineral oil are compared with those for water at two axial locations. Near the inlet (i.e. $z = 0.005$), there is almost no difference between the two temperature profiles of oil and water; however, at $z = 0.05$, which is in the middle of the thermally developing region, the temperature near the heated top wall for the oil is less than that for water. This phenomenon can be attributed to an efficient heat removal due to an increased velocity gradient near the heated top wall for the mineral oil.

Figure 3(b) shows the calculated dimensionless viscosity of the mineral oil in a thermally developing

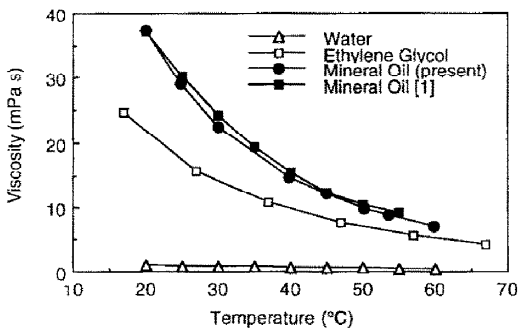

FIG. 2. Viscosities of three different fluids with temperature.

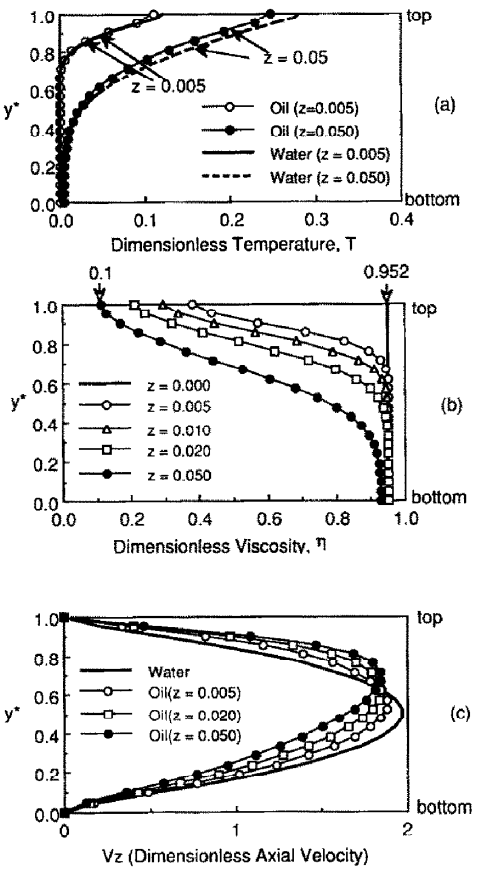

FIG. 3. (a) Dimensionless temperature profiles on mid-plane (i.e. $x^* = 0.5$) along the vertical (y) direction in a 2:1 rectangular duct with top-wall-heated, (b) dimensionless viscosity profiles on mid-plane (i.e. $x^* = 0.5$) along the vertical (y) direction in a 2:1 rectangular duct with top-wall-heated, (c) dimensionless axial velocities on mid-plane (i.e. $x^* = 0.5$) along the vertical (y) direction in a 2:1 rectangular duct with top-wall-heated.

flow. At the inlet (i.e. $z = 0$), the oil viscosity is uniform, having a value of 0.952 at the inlet temperature of 20°C. The viscosity of mineral oil near the heated top wall decreases dramatically with axial distance (i.e. $\eta = 0.952$ at $z = 0$ to $\eta = 0.1$ at $z = 0.05$), while the viscosity at the bottom wall almost remains unchanged.

In order to delineate the effect of variable viscosity on the velocity profiles in the thermally developing flow field, Fig. 3(c) shows velocity profiles on the mid-plane (i.e. $x^* = 0.5$) at four different axial locations (i.e. $z = 0.005$, 0.02, 0.04 and 0.05), where $y^* = 1.0$ refers to the heated top wall, and $y^* = 0$ refers to the unheated bottom wall. Obviously, the reduction of the viscosity causes a much steeper velocity gradient with increasing axial distance for the mineral oil than for water. The fully developed parabolic velocity profile (i.e. a solid curve) for water is shown as a reference in Fig. 3(c). The location of the maximum velocity is found to shift from the center of the rectangular duct at the inlet (i.e. $y^* = 0.5$) toward the heated top wall with increasing axial distance.

The axial distributions of bulk and top wall temperatures for the mineral oil and water are depicted in Fig. 4(a). The top wall temperature represents a space-averaged mean wall temperature. Due to the increase of velocity gradients near the heated top wall, the wall temperatures for the mineral oil are much lower than those for water, and the bulk temperatures for the mineral oil are slightly higher than those for water.

Figure 4(b) shows the axial distribution of the wall

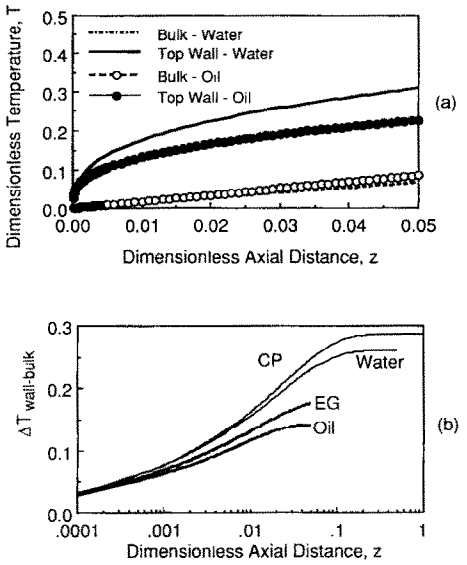

FIG. 4. (a) Dimensionless bulk and mean-wall temperature profiles along the dimensionless axial distance, z, and (b) differential temperatures between wall and bulk, $\Delta T_{\text{wall-bulk}}$, along the dimensionless distance. Thermal entrance lengths for CP, water, EG, and oil can be seen as the locations where $\Delta T_{\text{wall-bulk}}$ reaches respective plateau values. CP = constant property, EG = ethylene glycol.

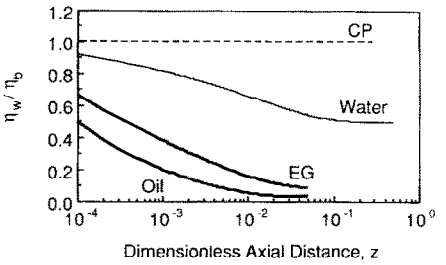

FIG. 5. Viscosity ratio vs dimensionless axial distance, z, for four different fluids.

and bulk temperature difference, $\Delta T_{\text{wall-bulk}}$, for mineral oil, ethylene glycol (EG), water, and a constant property fluid. Note that a thermally fully developed flow is obtained when $\Delta T_{\text{wall-bulk}}$ reaches a plateau value. The results, given in Fig. 4(b), clearly indicate that the thermal entrance lengths, L_{th}^+, for the above four fluids in the top-wall-heated rectangular duct are in the range of $0.03 \sim 0.2$, and the variable viscosity of the temperature-dependent fluids yields shorter thermal entrance lengths than for constant property fluid. For example, the mineral oil, the most temperature-dependent fluid included in the study, shows the shortest dimensionless thermal entrance length.

Figure 5 presents the viscosity ratio at the top wall and bulk fluid temperatures, η_w/η_b, along the axial distance. Approaching the end of a thermal entrance length, the viscosity ratio reaches an asymptotic value for each fluid. The smallest asymptotic value of the viscosity ratio is shown for the mineral oil.

In order to see the correlation between $f * Re$ and the dimensionless axial distance, z, the profile of $f * Re$ is presented along the axial distance in Fig. 6(a). At

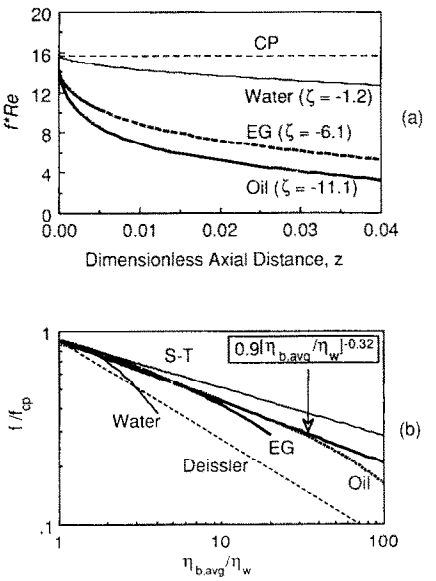

FIG. 6. (a) Product of the Fanning friction factor and the Reynolds number along the dimensionless axial distance, z, and (b) relative Fanning friction factor vs viscosity ratio. S-T = Sieder and Tate [5].

the inlet, $f * Re$ has a value of 15.53 and exponentially decreases with the axial distance. The higher the absolute value of ζ is, the more significantly the friction factor decreases.

Figure 6(b) shows the ratio of the friction factor for variable viscosity fluids to that for a constant property fluid, f/f_{cp}, as a function of the viscosity ratio, $\eta_{b,avg}/\eta_w$. This parameter, $\eta_{b,avg}/\eta_w$, was used by Sieder and Tate [5]. The subscript 'cp' indicates a value for a constant property fluid. In the thermally developing region, the friction factor ratios in the thermally developing region correlate well with the following equation:

$$\frac{f}{f_{cp}} = 0.9(\eta_{b,avg}/\eta_w)^{-0.32}. \quad (18)$$

The new correlation equation yields friction factor results that are between Sieder and Tate's correlation ($m = 0.25$) and Deissler's ($m = 0.54$). The discrepancy between the present results and Sieder and Tate's can be attributed to different thermal boundary conditions; i.e. Sieder and Tate's had a constant wall temperature condition, T, whereas the present study used a uniform asymmetrical wall heat flux condition, $H1(1L)$. In the thermally fully developed region, each curve in Fig. 6(b) deviates from the present prediction. Equation (18) is limited to the thermally developing region.

Figure 7 shows that the exponents, m, for friction factors in equation (2) are slightly increasing along the dimensionless axial distance even in the thermally developing region. The present results of m are compared with the results of Shannon and Depew [8] indicated by (S-D) and Yang [7]. The exponent values, m, reported by Shannon and Depew ranged from 0.510 to 0.635. The present values are generally found to be smaller than Yang's and Shannon and Depew's results but larger than Sieder and Tate's value. The m values of Shannon and Depew which were obtained using a thermal boundary condition similar to that of the present study (i.e. H_1) shows a trend similar to the present results. The difference between the previously reported values [7, 8] and the present result can probably be attributed to the different form of viscosity–temperature functions employed and to different Prandtl numbers of three test fluids, as given in Table 1.

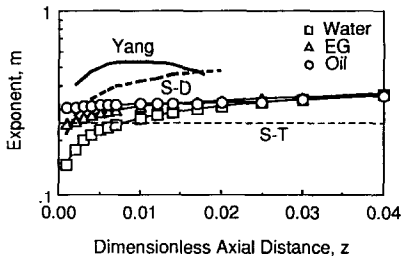

FIG. 7. The exponent m for friction factor along the dimensionless axial distance, z, in thermally-developing region. S-T = Sieder and Tate [5], S-D = Shannon and Depew [8].

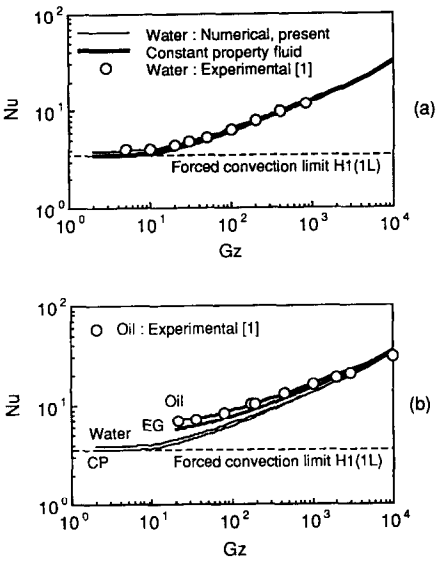

FIG. 8. The comparison of the present numerical laminar heat transfer results of water and oil with experimental results in a 2:1 rectangular duct with top-wall-heated. Heat transfer results of EG. and CP are given for comparison.

In order to examine the effect of variable viscosity on laminar heat transfer for water, the local Nusselt numbers are compared in Fig. 8(a), which shows 10% heat transfer enhancement for water compared with the results of constant property fluid, and also gives excellent agreement with experimental results for water reported by Xie and Hartnett [1]. In addition, the present calculation yields a Nusselt number of 3.54, which is identical to the forced convection limit [$H1(1L)$] in the thermally fully developed region in a 2:1 rectangular duct.

In order to quantify the overall effect of variable viscosity of the fluids on the laminar heat transfer performance in a top-wall-heated rectangular duct, Fig. 8(b) presents the local Nusselt numbers against the Graetz number. Present results calculated with variable viscosity oil give excellent agreement with corresponding experimental results for oil reported by Xie and Hartnett [1]. The Nusselt number for oil ($\zeta = 11.1$) is almost identical to the previous analytical results obtained for glycerin ($\zeta = 11.1$) [3] which can be attributed to the same ζ value. The Nusselt number is found to increase by 40–50% for oil (or glycerin) and by 70–80% when compared with those of constant property fluid. The laminar heat transfer enhancement can be attributed to the decrease of the viscosity near the heated top wall, which brings out the significant increase in velocity gradients and subsequent decrease in fluid temperatures near the top wall, rendering the overall increase in the local heat convection performance.

From the results given in Figs. 8(a) and (b), we conclude that the constant viscosity-variation parameter, ζ, is directly related to heat transfer enhancements; i.e. the higher ζ a fluid has, the larger the heat

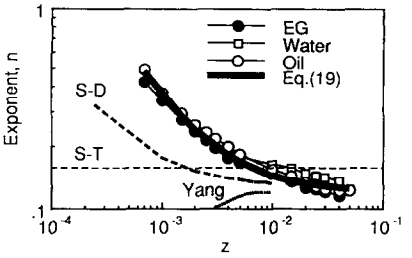

FIG. 9. The exponent n for heat transfer along the dimensionless axial distance, z.

transfer enhancement that will be produced. In general, the effect of temperature-dependent fluids on the laminar heat transfer is more significant in a non-circular duct than in a circular duct because in the latter a symmetric thermal boundary condition must be used and the effect of variable viscosity on heat transfer cannot be capitalized.

Figure 9 compares the exponent n for heat transfer correlation, equation (1), with the widely-accepted values of Sieder and Tate (S-T), Yang, and Shannon and Depew. As Bergles [14] pointed out, there was a rather generous distribution of the data about the chosen correlation of Sieder and Tate. Yang [7] reported that the n value was 0.11 for both the thermally developing and the thermally fully developed region. The present results shown in Fig. 9 indicate that the value of exponent n for heat transfer asymptotically approaches 0.12 in the thermally fully developed region. In the entry region the present n value is considerably larger than Sieder and Tate's value. Shannon and Depew, using their experimental heat transfer results obtained in the thermally developing region, reported a trend similar to the present results, although the magnitudes of n values were consistently smaller than the present values. The difference between the results of Shannon and Depew and the present results may be attributed to different thermal boundary conditions. The former used a symmetric thermal boundary condition, H_1, whereas the present study used an asymmetrical thermal boundary condition, $H1(1L)$.

As demonstrated in Fig. 9, the correlation of Sieder and Tate, as well as all the previously reported correlations (i.e. the ones shown in ref. [17]), fails to predict the laminar heat transfer in the thermally developing region. Therefore, a new correlation is proposed which covers both thermally developing and thermally fully developed regions:

$$n = n_\infty + \frac{Gz}{4000} \tag{19}$$

where n_∞ is 0.12, an asymptotic value of n in the thermally fully developed region as the Graetz number approaches zero. This correlation includes the effect of the Graetz number on the heat transfer enhancement and predicts the n values within 5% for the three fluids whose Prandtl numbers range from 7 to 15000. In the thermally developing region, the second term on the right hand side of equation (19) plays an important role, whereas in the thermally-fully-developed region, the second term on the right hand side becomes negligibly small; thus equation (19) reduces to a commonly used correlation form.

6. CONCLUSION

The present numerical calculations with three different fluids of variable viscosity were conducted under the assumption of an axially parallel flow in a top-wall-heated 2:1 rectangular duct, in which the effect of any secondary flow on heat transfer was excluded. The present numerical results of local Nusselt numbers for oil which give excellent agreement with recent experimental results [1], showed 70–80% enhancement over those of a constant property fluid and 40–50% enhancement over water. The heat transfer enhancement observed in the present study was achieved not because of the secondary flow at the corner but because of the steep velocity gradient associated with the decrease in the viscosity of fluids near the heated top wall. The study proposes a new correlation for the laminar heat transfer at the heated top wall in a 2:1 rectangular duct, which covers both thermally-developing and thermally fully developed regions. A temperature-dependent viscous fluid such as mineral oil or ethylene glycol can be used for the purpose of heat transfer enhancement in electronic cooling and compact heat exchangers, where uneven thermal boundary conditions with non-circular ducts are commonly utilized.

Acknowledgement—The authors wish to thank Messrs James M. Radka, Wayne Harmening and Don Schnorr of General Electric for their support of the present work.

REFERENCES

1. C. Xie and J. P. Hartnett, Influence of variable viscosity of mineral oil on laminar heat transfer in a 2:1 rectangular duct, *Int. J. Heat Mass Transfer* **35**, 641–648 (1992).
2. F. P. Incropera and D. P. DeWitt, *Fundamentals of Heat and Mass Transfer* (3rd Edn). Wiley, New York (1990).
3. N. S. Lyutikas and A. A. Zhukauskas, An investigation of the influence of variable viscosity on laminar heat transfer in a flat duct, *Int. Chem. Engng* **8**(2), 301–310 (1968).
4. H. W. Butler and D. E. McKee, An exact solution for the flow of temperature-dependent viscous fluids in heated rectangular ducts, *J. Heat Transfer* **95**, 555–557 (1973).
5. E. N. Sieder and G. E. Tate, Heat transfer and pressure drop of liquids in tubes, *Ind. Engng Chem.* **28**(12), 1429–1435 (1936).
6. R. G. Deissler, Analytical investigation of fully developed laminar flow in tubes with heat transfer with fluid properties variable along the radius, NACA TN 2410, Washington, D.C. (July 1951).
7. K. T. Yang, Laminar forced convection of liquids in tubes with variable viscosity, *J. Heat Transfer* **84**, 353–362 (1962).
8. R. L. Shannon and C. A. Depew, Forced laminar flow

convection in a horizontal tube with variable viscosity and free-convection effects, *J. Heat Transfer* **91,** 251–258 (1969).
9. R. Oskay and S. Kakaç, Effect of viscosity variations on forced convection heat transfer in pipe flow, *METU J. Pure Appl. Sci.* **6**(2), 211–230 (1973).
10. F. L. Test, Laminar flow heat transfer and fluid flow for liquids with temperature-dependent viscosity, *J. Heat Transfer* **90,** 385–393 (1968).
11. D. E. Rosenberg and J. D. Hellums, Flow development and heat transfer in variable-viscosity fluids, *Ind. Engng Chem. Fund.* **4,** 417–426 (1965).
12. D. R. Oliver and S. S. Rao, Heat transfer to viscous Newtonian liquids in laminar flow in straight horizontal circular tubes, *Trans. I.Ch.E.* **56,** 62–66 (1978).
13. S. D. Joshi and A. E. Bergles, Analytical study of laminar flow heat transfer to pseudoplastic fluids with uniform wall temperature, *A.I.Ch.E. Symposium Series* **77**(208), 114–122 (1981).
14. A. E. Bergles, Experimental verification of analyses and correlation of the effects of temperature-dependent fluid properties on laminar heat transfers. In *Low Reynolds Number Flow Heat Exchanger* (Edited by S. Kakaç, R. K. Shah and A. E. Bergles), pp. 473–486. Hemisphere, New York (1981).
15. V. Preiningerova and P. H. G. Allen, Laminar flow entry length heat transfer with varying physical properties in simple and complex duct geometries, *Proceedings of The 5th International Heat Transfer Conference*, Vol. 3, NC5.4, pp. 188–192 (1974).
16. S. T. Hwang and S. W. Hong, Effect of variable viscosity on laminar heat transfer in a rectangular duct, *Chemical Engineering Progress Symposium Series* **66**(102), 100–108 (1970).
17. S. Kakaç, The effect of temperature-dependent fluid properties on convective heat transfer. In *Handbook of Single-phase Convective Heat Transfer* (Edited by S. Kakaç, R. K. Shah and W. Aung), Chap. 18, p. 18-8. Wiley, New York (1987).
18. W. K. Gingrich, Y. I. Cho and W. Shyy, Effect of shear thinning on laminar heat transfer behavior in a rectangular duct, *Int. J. Heat Mass Transfer* **35,** 2823–2836 (1992).
19. J. P. Hartnett and M. Kostic, Heat transfer to Newtonian and non-Newtonian fluids in rectangular ducts, *Adv. Heat Transfer* **19,** 247–256 (1989).
20. S. V. Patankar, *Numerical Heat Transfer and Fluid Flow*. Hemisphere, New York (1980).
21. C. Hirsch, Numerical computation of internal and external flows. In *Fundamentals of Numerical Discretization*, Vol. 1. Wiley, New York (1988).
22. W. Shyy, A study of finite difference approximations for steady state, convection dominated flow problems, *J. Comput. Phys.* **57,** 415–438 (1985).
23. R. S. Varga, *Matrix Iterative Analysis*. Prentice-Hall, Englewood Cliffs, New Jersey (1962).